The University of Sydney

Department of Civil Engineering
Sydney NSW 2006
AUSTRALIA

http://www.civil.usyd.edu.au/

Centre for Advanced Structural Engineering

Design Models for Thin-Walled Sections in Bending Containing Unstiffened Elements

Research Report No R820

Bambach M.R. BE
Rasmussen K.J.R. MScEng, PhD

May 2002

The University of Sydney

Department of Civil Engineering
Centre for Advanced Structural Engineering
http://www.civil.usyd.edu.au/

Design Models for Thin-Walled Sections in Bending Containing Unstiffened Elements

Research Report No R820

Bambach M.R. BE
Rasmussen K.J.R. MScEng, PhD

May 2002

Abstract:

This report presents a general design procedure for calculating the moment capacity of sections containing unstiffened elements under stress gradients. The method uses the design equations for calculating both elastic and plastic effective widths of unstiffened elements under stress gradients, based on plate test results, presented in a companion report. Current international design provisions allow the capacity of sections that contain unstiffened elements under stress gradients to be calculated on the basis of initiation of yielding in the section. This report presents non-iterative methods for the calculation of the capacity, when both elastic and plastic effective width equations are used to establish the effective section. The methods are shown to be in good agreement with experimental data of I-sections and plain channels in minor axis bending. Particular attention is given to the effect of both the elastic buckling coefficient used in the effective width method, and the use of inelastic considerations, on the bending capacity of sections that contain unstiffened elements under stress gradients. Specific design proposals are presented in the form of amendments to the current Australian standard for cold-formed steel structures.

Keywords:

Moment capacity, unstiffened elements, effective width, first yield, inelastic reserve, I-sections, channel sections

Copyright Notice

Department of Civil Engineering, Research Report R820
Design Models for Thin-Walled Sections in Bending Containing Unstiffened Elements

mbambach@civil.usyd.edu.au

Published by:
Department of Civil Engineering
The University of Sydney
Sydney NSW 2006
AUSTRALIA

May 2002

http://www.civil.usyd.edu.au

INTRODUCTION

Current specifications for the design of open thin-walled sections provide equations for determining the effective width of stiffened and unstiffened elements, and the ultimate capacity of the section is calculated from the effective section properties. However, for cross-sections in bending with unstiffened elements under stress gradients, current design provisions have been shown to be unduly conservative. In a companion report (Bambach and Rasmussen 2002b), results of 80 plate tests of unstiffened plate elements, under strain gradients varying from pure compression to pure bending, are presented. In an additional report (Bambach and Rasmussen 2002a), elastic and plastic effective widths are deduced from the plate tests, and design equations for calculating both elastic and plastic effective widths are presented. In using elastic effective widths, the stress distribution is assumed to be linear-elastic with the maximum stress at yield, whereas in using plastic effective widths, the stress distribution is assumed to be elastic-plastic with constant stress at yield over part of the cross-section, including the effective width.

In current international design provisions, cold-formed sections that contain stiffened elements under stress gradients may be designed based on inelastic reserve capacity, where the maximum compressive strain in the section may be assumed to be up to three times the yield strain. These design rules were largely a result of experimental investigations on the inelastic strength of cold-formed beams by Reck, Pekoz et al. (1975) and Yener and Pekoz (1985a). However, when sections contain unstiffened elements under stress gradients, current international design provisions specify that the capacity be calculated on the basis of initiation of yielding in the section. Recent experimental studies of I-sections and plain channels in minor axis bending by Chick and Rasmussen (1999), Rusch and Lindner (2001), Beale, Godley et al. (2001), Rhodes (2000) and (Yiu and Pekoz (2001), have shown that these sections often reach their ultimate capacity in the post-elastic range. The combination of using simplified calculations for the effective widths of unstiffened elements under stress gradients, and calculating the capacity based on elastic considerations, was shown to result in bending capacities that were up to 50% conservative for sections containing unstiffened elements under stress gradients (Chick and Rasmussen 1999).

This report presents non-iterative design models, whereby sections that contain unstiffened elements under stress gradients may be designed based on inelastic reserve capacity. Elastic and inelastic models are presented, to be used in conjunction with effective sections calculated using the elastic or the plastic effective width equations. The effect of the value used for the elastic buckling coefficient in the effective width method is also investigated. It is shown that a tiered approach is applicable as a general method, whereby the buckling coefficient may be calculated (conservatively) from the existing equations in Appendix F of the Australian standard for cold-formed steel structures AS/NZS 4600 (1996) (the same as those given in Table 4.2 of Eurocode 3 (1996), Part 1.3), or by using a rational buckling analysis on the whole section.

Finally, the design models are presented in the form of amendments to the current Australian standard for cold-formed steel structures AS/NZS 4600 (1996), and are verified against section test data for channel sections in minor axis bending. The exact method of calculating the capacity of sections from plate test data of unstiffened elements is reviewed, and the simplifications required for the design models are summarised.

BUCKLING COEFFICIENT

The slenderness ratio (λ) in the strength curves derived from the plate tests and presented in the companion report (Bambach and Rasmussen 2002a), is calculated from the elastic critical buckling stress (f_{cr}) in Equation 1. The buckling coefficient (k) used in the strength curves is calculated from the Finite Strip program THINWALL (Papangelis and Hancock 1995), using the asymptotic value found with large half-

wavelengths. This is the theoretical solution for a plate simply supported on three sides with the remaining longitudinal edge free. It is noted that the buckling coefficients given in Appendix F of AS/NZS4600 (1996) and Table 4.2 of Eurocode 3 (1996), Part 1.3, are approximately the same as these.

$$\lambda = \sqrt{\frac{f_y}{f_{cr}}} \tag{1}$$

$$f_{cr} = \frac{k\pi^2 E}{12(1-\upsilon^2)\left(\frac{b}{t}\right)^2} \tag{2}$$

It is well known however, that the stiffened and unstiffened elements that comprise a section interact, such that rotational restraint exists along the longitudinal edge. The unstiffened element of a section often has a higher elastic buckling stress than an unstiffened plate that is simply supported along the longitudinal edge, and the buckling coefficient is consequently larger. For instance, a simply supported unstiffened plate element in pure compression has a buckling coefficient of 0.425, and an unstiffened element in an I-section in compression may have a buckling coefficient of 0.7 (depending on the web slenderness). Similarly, a simply supported unstiffened plate element with compressive strain at the unsupported edge and zero strain at the supported edge has a buckling coefficient of 0.57, and an unstiffened element in an I-section under minor axis bending may have a coefficient of 1.4 (depending on the web slenderness).

The American and Australian specifications allow an unstiffened element under stress gradient to be treated as a uniformly compressed element, specifying that the buckling coefficient of 0.43 may be used. This produces very conservative results for the bending capacity. However, current Australian and European design standards allow for a tiered approach for unstiffened elements under stress gradients. The buckling coefficients for elements under stress gradients, simply supported along the longitudinal edge, are given in Appendix F of AS/NZS4600 (1996) and Table 4.2 of Eurocode 3 (1996), Part 1.3, (using a non-iterative approach), and the designer may use these in place of a buckling coefficient of 0.43. Alternatively, the designer may use a rational buckling analysis of the whole section to determine an accurate value of the buckling coefficient. Part 5 of the British standard BS 5950 (1990) also allows a tiered approach where a general equation may be used (conservatively), or curves for standard sections given in Appendix B (based on rational buckling analyses) may be used. The American standard AISI (1996) is the most conservative, specifying that the buckling coefficient for uniformly compressed elements of 0.43 be used. Computer programs such as the Finite Strip program THINWALL are readily available, and give an accurate value of the elastic buckling stress (and thus the buckling coefficient). While it is possible to produce equations for the buckling coefficient for specific cases, many cold-formed sections have complicated geometries, and the tiered approach allowing a rational buckling analysis works well as a general design method. The design method proposed in this paper uses the same tiered approach as used in the Australian and European standards for calculating the elastic buckling coefficient, where the designer may calculate the buckling coefficient (conservatively) from Appendix F of AS/NZS4600 (1996) and Table 4.2 of Eurocode 3 (1996) Part 1.3 (Table 1), or use a rational buckling analysis of the whole section. In this report, both tiers are analysed in the verification of the proposed method.

EXACT CALCULATION OF THE MOMENT CAPACITY OF A CHANNEL SECTION USING THE PLATE TEST RESULTS FOR THE UNSTIFFENED ELEMENT

If one assumed that graphs of force and moment were available for any strain gradient (ψ) for all plate elements of a cross-section, as exemplified in Fig. 1c, it would be possible to calculate the moment-

curvature graph for the cross-section and from this determine the ultimate moment capacity. The procedure would be as follows:

1. Select a value for the maximum strain in the section (ε_{max_1}) and determine the strain gradient for the section (ψ) by finding the neutral axis position from Equation 3.
2. Select the appropriate plate tests that correspond to the strain gradient (Figure 1b), and calculate the effective width at the specified maximum strain in the section of ε_{max_1} (this assumes plate test results are available for an infinite number of different strain gradients, whereas only discrete values of strain gradients have actually been tested (Bambach and Rasmussen 2002a), and that the force and moment have been converted to an effective width and associated eccentricity, which is easily achieved).
3. Calculate the new strain gradient for the section, select the appropriate plate tests that correspond to this strain gradient and calculate the new effective width at the specified maximum strain in the section of ε_{max_1}.
4. Iterate until the correct effective section is established (Figure 1a), producing the strain gradient (ψ_1) for iteration 1 and effective width at the specified maximum strain in the section of ε_{max_1}, calculated from the plate test corresponding to ψ_1 (Figure 1c).
5. Calculate the moment in the section (M_{s_1}) from Equation 4 and the curvature in the section (κ_1) at the specified maximum strain in the section of ε_{max_1} (Equation 5).
6. Select an incrementally higher value for the maximum strain in the section (ε_{max_2}) and repeat steps 2-5 to calculate the moment in the section (M_{s_2}) and the curvature in the section (κ_2).
7. Repeat until a sufficiently detailed Moment-Curvature plot has been established (Figure 2), and determine the ultimate moment capacity for the section (M_u) as the maximum moment.

$$\int_A x dA = 0 \tag{3}$$

$$M_s = \int_A \sigma x dA \tag{4}$$

$$\kappa = \frac{\varepsilon_{max}}{b_c} \tag{5}$$

Within the limitation that this procedure assumes negligible interaction between plate elements in the ultimate limit state, it can be described as exact. It is, however, not suitable for design purposes.

SIMPLIFICATIONS FOR DESIGN PURPOSES

To develop a simple design procedure, the assumption will first be made that the strain distribution on a given element in the ultimate condition is close to that observed at ultimate in the plate tests. The assumption allows the effective width and eccentricity to be derived from the ultimate values of force and moment, as it was done in Bambach and Rasmussen (2002a). The assumption has been shown to be accurate for tests on I-sections and channel sections in minor axis bending. For the strain gradients encountered in these tests, the ultimate strain was of the order of two to three times the yield strain.

A rational procedure would now be as follows (here demonstrated for a channel section in minor axis bending):

Determine the stress gradient (ψ_1) based on the gross section (Figure 3a) and from this the buckling coefficient (k) and the effective width (b_e) and its eccentricity (*ecc2*) (Figure 3b). In order to calculate the stress distribution, the strain distribution is assumed to be linear with a maximum strain on the effective

section of $n\varepsilon_y$, where n should be consistent with the values observed in tests of sections, typically 2 or 3. The stress distribution can then be determined, as shown in Figure 3c. It will be elastic-plastic if $n>1$, or linear-elastic if $n=1$ is assumed. It then needs to be checked whether the assumed neutral axis position is correct by calculating the resultant axial force ($\int\sigma dA$). If not negligible, the neutral axis position is changed and the calculation process repeated. This involves new values of stress gradient (ψ), buckling coefficient (k), effective width (b_e), and eccentricity ($ecc2$). Once the neutral axis has been established, the moment capacity can be determined using Equation 4.

Several issues arise in applying this procedure:

1. While tests have shown that the maximum strain on the section may be several times the yield strain in the ultimate limit state, design of non-fully effective cross-sections is usually premised on linear-elastic stress distributions which implies that the maximum strain should be limited to the yield strain ($n=1$). It will be shown that accounting for inelastic stress distributions is especially important for cross-sections that contain elements capable of significant in-plane yielding in tension, such as I-sections in minor axis bending.
2. The assumed strain distribution determines the type of effective width to use: If the maximum strain is taken as two or three times the yield strain, the stress distribution on the effective width is likely to be uniform at yield, and the use of plastic effective widths is appropriate. However, if the maximum strain is assumed to be limited to the yield strain, then the stress distribution is linear and elastic effective widths are appropriate.
3. The procedure is iterative because the strain gradient changes after each iteration. While iterating is conceptually correct, a direct design procedure can be achieved if the neutral axis position is assumed to be that of the gross cross-section, implying that only the first iteration is necessary.

These issues will be addressed in the sections following by comparing test strengths of channels and I-sections with design strengths obtained using elastic and inelastic stress distributions, plastic and elastic effective widths, as well as iterative and direct design procedures.

EXPERIMENTS ON I-SECTIONS AND CHANNELS IN MINOR AXIS BENDING

The results of experimental work published by Chick and Rasmussen (1999) and Rusch and Lindner (2001) on I-sections in minor axis bending, and Beale, Godley et al. 2(001), Yiu and Pekoz (2001), Rhodes (2000), El Mahi (1985) and Rhodes (1985) on plain channel sections in minor axis bending, are analysed here in order to verify the proposed effective width method. All tests were four point bending tests, except those by Chick and Rasmussen which were performed in a dual actuator rig whereby end rotations were controlled directly to produce uniform moment. No global instabilities such as lateral torsional buckling occurred in the tests. Dimensions of sections analysed are given in Tables 1,2.

The experimental studies by Chick and Rasmussen (1999) and Rusch and Lindner (2001) on I-sections in minor axis bending, and Beale, Godley et al. (2001), Rhodes (2000), and Yiu and Pekoz (2001) on plain channel sections in minor axis bending, have shown that these sections often exhibit post-elastic behavior. For example an I-section in minor axis bending with flange slenderness 1.0 (Equation 1) tested by Chick (1997) reached a curvature of 2.1 times the yield curvature at ultimate, and a similar section with flange slenderness of 1.44 tested by Rusch and Lindner (2001) reached a curvature of approximately 3 times the yield curvature. The yield curvature is calculated as the yield strain (at the flange tip) divided by the flange width. Experiments on plain channels and channels with inclined flanges in minor axis bending (producing compression at the flange tip) by Rhodes (2000) showed full plastic capacity for b/t ratios less than 15, and post-elastic capacity up to approximately 30. A similar result was found by Beale, Godley et al. (2001) from

tests on plain channels in minor axis bending. Yiu and Pekoz (2001) proposed that plain channels in minor axis bending (producing compression at the flange tip) exhibit post-elastic capacity for flange slenderness ratios less than 0.859.

COMPARISION BASED ON INITIATION OF YIELDING

The proposed method for plastic effective widths (Bambach and Rasmussen 2002a) is first compared with the section data by calculating the ultimate limit state capacity based on the initiation of yielding in the effective section. Using the section properties in Tables 1,2 and the proposed effective width equations, an effective section is established (Figure 4). It is noted that for unstiffened elements that have tension at the supported edge, for example plain channel sections in minor axis bending (causing the flange tip to be in compression), the proposed method gives the effective width of the *compressed portion* of the element. The portion of the element in tension in the gross section is assumed to be fully effective also. Initially, the effective width is calculated assuming that the ratio of the edge stresses is based on the gross section, such that no iteration is required. The elastic effective section properties are calculated, being the effective neutral axis (x_e) and the effective section modulus (Z_e). The stress distribution on the effective section is deduced by assuming elastic material behavior, and maximum strain in the effective section of the yield strain (Figure 4). The nominal section moment capacity may then be calculated as the moment of the stress blocks about the effective neutral axis (Equation 6), or from the effective modulus (Equation 7).

$$M_s = \int_A \sigma x dA \tag{6}$$

$$M_s = Z_e f_y \tag{7}$$

The nominal section moment capacities calculated at the point of initiation of yielding in the effective section are compared with test results in Figures 5,6. The moment capacities are non-dimensionalised with respect to the full plastic moment, and are plotted against the non-dimensionalised slenderness parameter $(b_f/t)\sqrt{(f_y/E)}$. The effect of the value used for the buckling coefficient is represented in the curves by plotting a curve for both tiers, i.e. if one calculates the effective section assuming the unstiffened element has the longitudinal edge simply supported, or if one calculates the effective section using a buckling coefficient calculated from a rational buckling analysis. The values for the buckling coefficient given in AS/NZS4600 (1996) Appendix F (the same as those in Eurocode 3 (1996), Part 1.3) are used for the former, and the Finite Strip program THINWALL is used for the latter ('k from rational analysis' in Figures 5,6), and in both cases the edge stresses are calculated on the basis of the gross section.

For I-sections in minor axis bending, solutions using AS/NZS4600 (1996) with the buckling coefficient calculated from both Appendix F and using THINWALL are included for comparison (Figure 5). The solutions using the proposed method are similar to those using AS/NZS4600 (1996). The solution using AISI (1996) is also included, and is shown to be quite conservative (due to the use of a buckling coefficient of 0.43). It can be clearly seen that methods based on initiation of yielding in the section do not accurately predict the capacity. This is a result of the fact that, a) in actuality, the sections are in the post-elastic range at ultimate, which produces an elastic-plastic stress distribution in the tension-loaded part of the cross-section, and b) in the compression loaded part of the cross-section, the stress on the effective width is assumed to be linearly decreasing from yield, whereas the stress was assumed constant at yield in deriving the plastic effective width equations.

For channel sections in minor axis bending (causing the flange tip to be in compression), solutions using AS/NZS4600 (1996) with the buckling coefficient calculated from both Appendix F and THINWALL are included in Figure 6, as are solutions using BS5950 (1990) Part 5 (buckling coefficient given by Equation

9), AISI (1996), and Equations 8,9 proposed by Rhodes (2000) (the elastic solution only is printed here). Equation 9 is the accurate solution for buckling coefficients of channels given in Appendix B of BS5950. Using the proposed method and a buckling coefficient from THINWALL, good correlation with the test data is found above a value for $(b_f/t)\sqrt{(f_y/E)}$ of 1.35. Below this value the proposed curve is conservative, since the sections exhibit some post-elastic capacity, and below approximately 0.52, experimentally they reach full plastic capacity. Again, a method based on initiation of yielding in the section does not accurately predict the capacity.

$$\frac{b_e}{b} = 0.9\lambda^{-\frac{2}{3}} \tag{8}$$

$$k = \frac{3.4}{2 + \frac{h}{1+h}} \tag{9}$$

As mentioned previously, the capacities in Figures 5,6 were calculated by basing the edge stresses on the gross section for the purpose of effective width calculations, such that no iteration is required to calculate the effective section. It is shown in Figure 7 that for channel sections, this method is conservative compared with the more realistic method of iterating to calculate the effective section, such that the edge stresses are calculated on the basis of the effective section. The calculated capacity increases with iteration due to the fact that the calculated effective width increases as the neutral axis position shifts towards the web (after each iteration) (see Figure 8 in Bambach and Rasmussen 2002a). However, on average the difference is small (3%), and it may be concluded then, that iterations are not required.

ANALYSIS OF THE EFFECTIVE SECTION IN THE POST-ELASTIC RANGE

Where the ultimate limit state capacities calculated are conservative in Figures 5,6, it is proposed that the assumption that the ultimate limit state is the point at which the maximum strain in the effective section reaches the yield strain is conservative. A method is established here for calculating the capacity of the effective section when the maximum strain on the effective section exceeds the yield strain. It is noted that the effective section dimensions are not recalculated as the maximum strain is increased (and the strain gradient changes), such that the effective section need only be calculated once. This approach simplifies the process for design purposes. Initially, a value for the maximum compressive strain in the effective section is assumed ($n\varepsilon_y$). A value for the position of the plastic neutral axis is then assumed (x_p), and a stress distribution calculated for this neutral axis position. The total forces in tension and in compression are calculated from the stress distribution. If the net force is not equal to zero (i.e. Equation 10 is not satisfied), a new plastic neutral axis position must be chosen, and the process repeated. When the section is in equilibrium, the moment capacity (calculated from the moment of the stress blocks about the plastic neutral axis – Equation 6) is calculated, and this is the moment capacity for when the section has a maximum strain of n times the yield strain. If we repeat the process with a larger value of n, we find the moment capacity at this increased strain, and so on. The process may be repeated until the moment capacity is equal to that found in the experiment for a given section, and a good estimate is thus found of the maximum strain in the section at ultimate. This method was carried out on the experimental results of the aforementioned authors on I-sections and channels in minor axis bending. Sample spreadsheet calculations are given in Appendix A.

$$\int_A x dA = 0 \tag{10}$$

Table 3 shows the results of this process for I-sections in minor axis bending. Since the results are being compared to experimental data, the exact buckling coefficient was calculated from THINWALL. Of the six

sections analysed, five had a maximum compressive strain on the *effective* section of more than three times the yield strain. While the maximum compressive strain in the *effective* section at ultimate (C_y ε_y) in the experiments is known for only two specimens, both compare well with the C_y values calculated here. The C_y value for specimen 5800-5 tested by Chick (1997) is 2.3, and the calculated value is 2.3. The C_y value for specimen B013 tested by Rusch and Lindner (2001) is approximately 3, and the calculated value is 3.1.

SHIFT OF THE EFFECTIVE NEUTRAL AXIS

An interesting result of the analysis was the fact that the plastic effective neutral axis was very close to the elastic effective neutral axis (Table 3). The effective neutral axis shifted very little as the strain on the effective section increased in the post-elastic range to the ultimate condition. As a percentage of the flange width, the average shift is approximately 1%. If the elastic neutral axis position is used in the spreadsheets for I-sections at the ultimate strain instead of the plastic value, the net force on the section is not exactly equal to zero, however the average decrease in the moment capacity is only 0.26% (Table 3). In the inelastic range then, it is proposed that a reasonable assumption of the ultimate moment capacity may be achieved by using the elastic effective neutral axis position, and applying a maximum compressive strain on the effective section (C_y ε_y) of three times the yield strain, for I-sections in minor axis bending (Figure 8). The moment capacity is then calculated from the moment of the stress blocks about the elastic effective neutral axis (Equation 6), using an elastic-perfectly plastic assumption to determine the stress distribution. The advantage of such a solution is that the procedure is non-iterative. As shown in the right-most column of Table 1, the procedure is very accurate.

The same process was applied to plain channel sections in minor axis bending (causing the flange tip to be in compression), and a similar result was found (Table 4). Again, it is noted that the effective section dimensions are not recalculated as the maximum strain is increased, such that the effective section need only be calculated once. As a percentage of flange width, the average shift of the neutral axis for the sections studied is 2%. If the elastic neutral axis position is used in place of the plastic neutral axis position, an average increase in the moment capacity of 4.3% occurs. Sections with a $(b_f/t)\sqrt{(f_y/E)}$ value of less than 1.35 in Figure 6 demonstrated some post-elastic capacity, and the maximum value of $(b_f/t)\sqrt{(f_y/E)}$ for sections that are fully effective is 0.34 (determined from the proposed effective width equations). It is proposed that a reasonable assumption of the ultimate capacity may be achieved by using the elastic effective neutral axis, and applying a maximum compressive strain on the effective section of $C_y\varepsilon_y$ (Figure 9), where C_y is calculated as a linear interpolation between C_y=1 at $(b_f/t)\sqrt{(f_y/E)}$=1.35, and C_y=3 at $(b_f/t)\sqrt{(f_y/E)}$=0.34. The moment capacity is calculated using Equation 6. Again, the procedure has the advantage of being non-iterative. It is noted that the values of the shift of the neutral axis and consequent change in moment capacity for channel sections presented in Table 4 are calculated at the proposed values of C_y, whereas for I-sections they are calculated at the value of C_y that produces a moment capacity that matches the test results. This is due to the fact that calculations show that for the stockier sections studied, the test capacities exceed the full plastic capacity of the effective section (calculated using the plastic effective width equations). Consequently, the proposed method is slightly conservative when compared with the test capacities, for the stockier sections.

A tiered approach is proposed, where a designer may calculate the section moment capacity based on initiation of yielding (conservatively), or use a higher tier approach based on inelastic reserve capacity, the non-iterative procedure for which is outlined below.

DESIGN EQUATIONS FOR THE NOMINAL SECTION MOMENT CAPACITY BASED ON INELASTIC RESERVE CAPACITY

It is proposed that when the plastic effective width equations are used to calculate the effective width of an unstiffened element under a stress gradient, the nominal section moment capacity (M_s) shall be determined by applying a maximum compression strain of $C_y\varepsilon_y$ on the effective section, assuming that the plastic neutral axis of the effective section is at the same position as the elastic neutral axis of the effective section. The yield strain is calculated as:

$$\varepsilon_y = \frac{f_y}{E}$$

The compression strain factor (C_y) shall be determined as follows:

For unstiffened elements that form part of an I-section in minor axis bending:

$$C_y = 3$$

For unstiffened elements that form part of a channel-section in minor axis bending causing compression at the unsupported edge of the flange:

$$C_y = 3.67 - 1.98\frac{b_f}{t}\sqrt{\frac{f_y}{E}} \qquad \text{where } 1 \le C_y \le 3$$

For unstiffened elements that form part of a channel section in minor axis bending causing compression at the supported edge of the flange:

$$C_y = 3$$

For all other unstiffened elements: $C_y = 1$

COMPARISON BASED ON INELASTIC RESERVE CAPACITY

For sections with maximum compressive strain at the unsupported edge of the unstiffened element, the proposed equations for plastic effective widths and nominal section moment capacity based on inelastic reserve capacity are compared with the experiments by the aforementioned authors on I-sections in minor axis bending (Figure 10), and plain channel sections in minor axis bending (causing the flange tip to be in compression) (Figure 11). In the calculation of the effective section, both the buckling coefficient calculated from AS/NZS4600 (1996) Appendix F (the same as those in Table 4.2 of Eurocode 3 (1996), Part 1.3), and the exact value calculated from the higher tier approach using THINWALL are used. Good agreement is found between the experiments and the proposed method, when the higher tier approach for the buckling coefficient is used. It is noted that solutions from international design codes are not included in Figures 10,11, since all codes specify that the maximum compressive strain on unstiffened elements is limited to the yield strain (thus the solutions are the same as those in Figures 5,6). The moment values are compared with test values in Tables 1,2. It is clear from these analyses that while the method of calculation of the elastic buckling coefficient has a significant effect on the bending capacity, one can obtain very good agreement with tests when using the rational estimation of the buckling coefficient in the proposed design method based on inelastic reserve capacity. For the I-sections, the increase in moment capacity compared to the elastic procedure (Figure 5) is derived mainly from modeling the stress distribution in the tension-loaded flanges as elastic-plastic, rather than linear-elastic.

For sections with maximum compressive strain at the supported edge of the unstiffened element, the proposed equations for plastic effective widths (Bambach and Rasmussen 2002a) and nominal section moment capacity based on inelastic reserve capacity are compared with the experiments by Enjily, Godley et al. (1999) on plain channel sections in minor axis bending (causing the flange tip to be in tension) in Figure 12. The design rules for stiffened elements in compression in AS/NZS4600 (1996) (the same as those

in the AISI (1996) specification) were used to calculate the effective width of the web, and for all section geometries the flanges were found to be fully effective (when both Appendix F and rational analyses were used to calculate the buckling coefficient). The method allows a maximum compressive strain of three times the yield strain on the unstiffened element, with the maximum tensile strain exceeding the yield strain. Figure 12 shows the method to be slightly conservative when compared with the test results, however a satisfactory estimation of the bending strength is achieved for all section geometries.

DESIGN EQUATIONS FOR THE NOMINAL SECTION MOMENT CAPACITY USING THE ELASTIC EFFECTIVE WIDTH METHOD

It has been shown that plastic effective widths (situated at an eccentricity to the supported edge) satisfy exactly the ultimate force and moment values that were obtained in the plate tests, and can be used in conjunction with inelastic considerations to accurately predict the minor axis moment capacity of I-sections and plain channels. It is recognised however, that all international design standards are based on the assumption of elastic effective widths situated adjacent to the supported edge, and an elastic effective width model of this nature may be more appropriate to incorporate into current standards than a plastic model. For this purpose, elastic effective widths adjacent to the supported edge were derived from the plate tests, and are presented in the companion report (Bambach and Rasmussen 2002a). The advantage of this model is that the effective width factor (ρ) multiplied by the gross element width (b) gives the effective width of the element measured from the supported edge, which is congruent with current standards. Examples of effective sections calculated with the elastic effective width equations are shown in Figure 13.

The elastic effective widths were derived from the ultimate force values from the plate tests, however due to the omission of the eccentricity from the supported edge, the ultimate moment values in the plate tests are underestimated by the elastic method. It is shown in Figure 14 that when the edge stresses are calculated on the basis of the effective section, such that iteration is required to establish the effective section, the elastic method is conservative compared with section test data, since the elastic effective widths underestimate the moment resistance. However, when the edge stresses are calculated on the basis of the gross section, such that no iteration is required, the calculated effective widths are larger and the elastic method predicts the section bending capacity well. It is proposed then, that the edge stresses may be calculated on the basis of the gross section for effective width calculations.

Since elastic effective widths are larger than plastic effective widths, when used in conjunction with the C_y values proposed for the plastic effective width method, the minor axis moment capacities exceed the test results for the studied I-sections and plain channels. The C_y values must be scaled down to be used with elastic effective widths. The following C_y values are proposed to calculate the maximum compressive strain on an effective section calculated using the elastic effective width equations, assuming that the plastic neutral axis of the effective section is at the same position as the elastic neutral axis of the effective section:

For unstiffened elements that form part of an I-section in minor axis bending:

$$C_y = 2$$

For unstiffened elements that form part of a channel-section in minor axis bending causing compression at the unsupported edge of the flange:

$$C_y = 3 - 2\frac{b_f}{t}\sqrt{\frac{f_y}{E}} \qquad \text{where } 1 \le C_y \le 2$$

For unstiffened elements that form part of a channel section in minor axis bending causing compression at the supported edge of the flange:

$$C_y = 2$$

For all other unstiffened elements: $C_y = 1$

The bending capacities calculated using a buckling coefficient calculated from THINWALL with the elastic effective width equations and the reduced C_y values are compared with section test results in Figures 15,16. The capacities calculated with the plastic effective width equations and unreduced C_y values (Figures 10,11) are reprinted in Figures 15,16 for comparison. Both methods are in good agreement with the test results. Also printed in Figures 15,16 are capacities calculated using a first yield approach, and it is shown that for both elastic and plastic effective widths, the first yield approach does not accurately predict the section test results.

The assumption that the elastic neutral axis of the effective section may be used in lieu of the plastic neutral axis was shown to have little effect on the bending capacity when using the plastic effective width equations. Calculations show that this assumption is also valid when using the elastic effective width equations. If the elastic neutral axis position is used in place of the plastic neutral axis position, an average decrease in the moment capacity of I-sections of 0.3% occurs, and an average increase in the moment capacity of channel sections of 4.3% occurs.

PROPOSED AMENDMENTS TO AS/NZS 4600

It has been shown that the plastic effective width model satisfies both the ultimate force and moment values from the plate tests on unstiffened elements, and gives a good approximation of the bending capacity of sections that contain unstiffened elements under stress gradients. The elastic effective width model satisfies the ultimate force from the plate tests, however underestimates the moment capacity of the plates due to the assumption that the effective width is adjacent to the supported edge. Consequently the elastic effective width model produces conservative estimates of the bending capacity of sections that contain unstiffened elements under stress gradients. It has been shown, however, that when the stress gradient is calculated on the basis of the gross section for effective width calculations, a reasonable estimation of the section bending capacity is achieved, since the effective widths calculated are larger. Since the elastic effective width adjacent to the supported edge model is in line with the existing effective width method used in AS/NZS4600 (1996), the amendments to Clause 2.3.2 of AS/NZS 4600 proposed in Appendix B are based on the elastic effective width model, assuming that the strain gradient is calculated on the basis of the gross section. The equations for the buckling coefficient in the proposed amendments are those that currently exist in Appendix F of AS/NZS4600, therefore Appendix F is no longer required, and allowance is made for a higher tier approach based on a rational elastic buckling analysis.

It has been shown that the bending capacities of sections that contain unstiffened elements under stress gradients may be calculated conservatively when the ultimate limit state of the section is taken as the point at which the maximum stress on the effective section is the yield stress. The amendments to Clause 3.3.2.2 of AS/NZS 4600 proposed in Appendix C allow the moment capacity of sections that contain unstiffened elements to be based on inelastic reserve capacity. The inelastic reserve capacity equations presented earlier in this report are modified such that the method is in line with the inelastic reserve capacity method for sections containing stiffened elements, where inelastic reserve capacity may only be applied to sections that are fully effective. The equations are also modified to include the parameter for the ratio of the edge stresses on the unstiffened element (ψ). This generalises the equations such that they may be used on any section that contains unstiffened elements with stress gradients, when that section is fully effective. The method constitutes a higher tier approach for sections that are fully effective.

The proposed effective width equations and inelastic reserve capacity allowance are verified against section test data for I-sections in minor axis bending (Figure 17), and plain channel sections in minor axis bending where the unsupported edge of the unstiffened element is in compression (Figure 18). It is shown in Figure 17 that the proposals are conservative compared with section test data for I-sections, due to the fact that the

inelastic reserve capacity may only be applied to fully effective sections in the proposed Clause 3.3.2.3, whereas it has been shown earlier in this report that the inelastic reserve capacity method must be applied to all sections in order to produce agreement with the tests. However, the proposals produce more accurate estimates of the bending capacity than does the Winter formula with a buckling coefficient of 0.43 (AISI (1996) in Figure 17). It is shown in Figure 18 that the proposals produce good agreement with section test data for channel sections, when the higher tiers are used. The lower tiers produce more accurate estimates of the bending capacity than does the Winter formula with a buckling coefficient of 0.43 (AISI (1996) in Figure 18).

CONCLUSIONS

In a companion report (Bambach and Rasmussen 2002a), a general design method is proposed for calculating effective widths of unstiffened elements under stress gradients, where either elastic or plastic effective width equations may be used. The tiered approach currently used in AS/NZS4600 (1996) for calculating the elastic critical buckling stress is suggested in this report, whereby a designer may (conservatively) use the buckling coefficient given in AS/NZS4600 Appendix F (the same as those in Table 4.2 of Eurocode 3 (1996), Part 1.3), or use a rational buckling analysis of the whole section. In the application of both methods, the edge stresses are calculated on the basis of the gross section. A design method for sections in bending where the unstiffened element is subjected to a stress gradient is proposed. An approach similar to that currently used in international codes for stiffened elements is suggested, whereby the nominal section moment capacity may be calculated based on initiation of yielding, or based on inelastic reserve capacity.

A method for calculating the moment capacity based on inelastic reserve capacity when plastic effective widths are used is presented, where the designer may assume that the maximum compression strain in the effective section is up to three times the yield strain. Good agreement is found between the method and experiments on I-sections and plain channel sections in minor axis bending. It is shown that there is negligible difference in capacity between calculating the edge stresses on the basis of the gross section or the effective section, for the purpose of effective width calculations. Iterations can be avoided by calculating the edge stresses on the basis of the gross section.

An alternative method for calculating the bending capacity based on inelastic reserve capacity when elastic effective widths are used is presented. The method allows the designer to use a maximum compression strain in the effective section of up to two times the yield strain. While the elastic effective width method underestimates the moment resistance, it is shown that good agreement with experiments on I-sections and plain channels in minor axis bending is achieved when the ratio of the edge stresses is based on the gross section, for the purpose of effective width calculations. The elastic effective width design model is presented in the form of proposed amendments to the current Australian standard for cold-formed steel structures.

REFERENCES

AISI (1996). *Specification for the Design of Cold-Formed Steel Structural Members*. Washington D.C., American Iron and Steel Institute.

AS/NZS 4600 (1996). *Australian/New Zealand Standard. Cold-Formed Steel Structures*. Sydney, Standards Australia.

Bambach, M.R. and Rasmussen, K.J.R. (2002a). "Elastic and Plastic Effective Width Equations for Unstiffened Elements".*Research Report, R819*. Sydney, Department of Civil Engineering, University of Sydney.

Bambach, M.R. and Rasmussen, K.J.R. (2002b). "Tests of Unstiffened Plate Elements under combined Compression and Bending".*Research Report, R818*. Sydney, Department of Civil Engineering, University of Sydney.

Beale, R.G., Godley, M.H.R. and Enjily, V. (2001). "A Theoretical and Experimental Investigation into Cold-formed channel sections in Bending with the Unstiffened Flanges in Compression." *Computers and Structures* **79**: 2403-2411.

BS 5950 (1990). *Structural use of Steelwork in Building. Part 5. Code of Practice for the Design of Cold Formed Sections*.

Chick, C.G. (1997). *Thin-Walled I-Sections in Compression and Bending*.PhD Thesis. Sydney, Sydney University.

Chick, C.G. and Rasmussen, K.J.R. (1999). "Thin-Walled Beam-Columns. 2:Proportional Loading Tests." *Journal of Structural Engineering, ASCE* **125**(11): 1267-1276.

El Mahi, A. (1985). *Behaviour of Unstiffened Elements in Bending*.M.S. Thesis. Glasgow, UK, University of Strathclyde.

Enjily, V., Godley, M.H.R. and Beale, R.G. (1999). "An Experimental Investigation into Cold-Formed Channel Sections in Bending". *Proc., International Conference on Advances in Steel Structures*, Elsevier.Teng, J.G.

Eurocode 3 (1996). *Eurocode 3: Design of Steel Structures, Part 1.3: General Rules - Supplementary Rules for Cold Formed Thin Gauge Members and Sheeting*. Brussels, European Committee for Standardisation, European Prestandard, ENV 1993-1-3.

Papangelis, J.P. and Hancock, G.J. (1995). "Computer Analysis of Thin-Walled Structural Members." *Computers and Structures* **56**(1).

Reck, H.P., Pekoz, T. and Winter, G. (1975). "Inelastic Strength of Cold-Formed Steel Beams." *Journal of the Structural Division, ASCE* **101**(ST11).

Rhodes, J. (1985). "Final Report on Unstiffened Elements". Glasgow, UK, University of Strathclyde.

Rhodes, J. (2000). "Buckling of Thin Plates and Thin-Plate Members". *Proc., Structural Failure and Plasticity, IMPLAST 2000*, Elselvier.Grzebieta, R.H.

Rusch, A. and Lindner, J. (2001). "Remarks to the Direct Strength Method." *Thin-Walled Structures* **39**: 807-820.

Yener, M. and Pekoz, T.B. (1985a). "Partial Stress Redistribution in Cold-Formed Steel." *Journal of Structural Engineering, ASCE* **111**(6).

Yiu, F. and Pekoz, T. (2001). "Design of Cold-Formed Steel Plain Channels. Final Report". Ithaca, USA, Cornell University.

Specimen	b_f (mm)	b_w (mm)	t (mm)	Yield stress (MPa)	M_{test} (kNm)	Proposed M/M_{test}	C_y
B009	50	80	1.9	228	1.75	0.970	3
B010	50	80	1.9	228	1.76		
B015	50	80	2	368	2.61	1.021	3
B016	50	80	2	368	2.59		
B005	75	80	1.9	230	3.32	0.972	3
B006	75	80	1.9	230	3.34		
B007	75	80	1.5	188	2.12		
B008	75	80	1.5	188	2.2		
B013	75	80	2	368	5.16	0.993	3
B014	75	80	2	368	5.13		
B003	100	80	1.9	230	5.55	0.924	3
B004	100	80	1.9	230	5.46		
B001	100	80	1.5	188	3.36		
B002	100	80	1.5	188	3.36		
B011	100	80	2	368	8.42	0.976	3
B012	100	80	2	368	8.36		
					Mean:	0.98	
					Standard Deviation:	0.032	

Table 1: I-sections in minor axis bending tested by Rusch and Lidner, compared with proposed inelastic method with plastic effective widths

Specimen	b_f (mm)	b_w (mm)	t (mm)	Yield stress (MPa)	M_{test} (kNm)	Proposed M/M_{test}	C_y
M9	8	30	1.6	232.5	0.023		*
M10	16	45	1.6	232.5	0.102		*
M11	24	60	1.6	232.5	0.228		*
M12	32	75	1.6	232.5	0.331	0.862	2.3
M13	40	90	1.6	232.5	0.383	0.922	2.0
M14	48	105	1.6	232.5	0.431	0.951	1.6
M15	56	120	1.6	232.5	0.474	0.975	1.3
M16	64	135	1.6	232.5	0.532	0.846	1
Q1	80	160	1.6	183	0.665	0.763	1
Q2	105	210	1.6	183	0.893	0.804	1
Q3	120	240	1.6	183	0.945	0.901	1
Q4	135	270	1.6	183	1.120	0.885	1
Q5	150	300	1.6	183	1.295	0.878	1
					Mean:	0.88	
					Standard Deviation:	0.064	

*Test values exceed the plastic moment, therefore no comparison is made

Table 2: Channels in minor axis bending (flange tip in compression) tested Beale et al. (2001), compared with proposed inelastic method with plastic effective widths

Rusch and Lindner (2001) Specimen	Value of C_y such that the moment matches the test result	Elastic effective neutral axis (mm)	Plastic effective neutral axis (mm)	Shift of the neutral axis as a percentage of the flange width	Decrease in capacity due to using the elastic effective neutral axis
B009	4.9	46.1	45.9	0.50%	0.34%
B015	2.5	44.8	43.9	1.77%	0.15%
B005	3.9	63.8	63.7	0.08%	0.03%
B013	3.1	62.1	61.7	0.48%	0.04%
B003	4.5	80.2	82	1.83%	0.83%
B011	3.4	78.2	78.8	0.64%	0.18%
			Mean:	0.88%	0.26%
			Standard Deviation:	0.73%	0.30%

Table 3 : I-sections in the post-elastic range, using plastic effective widths to establish the effective section

Specimen	Proposed value of C_y	Elastic effective neutral axis (mm)	Plastic effective neutral axis (mm)	Shift of the neutral axis as a percentage of the flange width	Increase in capacity due to using the elastic effective neutral axis
M12 _ _ a	2.3	6.03	4.30	5.41%	11.42%
M13 _ _ a	2.0	6.71	5.10	4.02%	7.80%
M14 _ _ a	1.6	7.12	6.20	1.91%	3.54%
M15 _ _ a	1.3	7.55	7.53	0.04%	0.04%
6 _ _ b	2.1	8.41	8.63	0.88%	0.75%
7 _ _ b	1.3	4.69	3.43	3.26%	9.18%
			Mean:	2.02%	4.26%
			Standard Deviation:	1.64%	4.10%

[a] Beale et al. (2001)

[b] El Mahi and Rhodes (1985)

Table 4: Channels in the post-elastic range, using plastic effective widths to establish the effective section

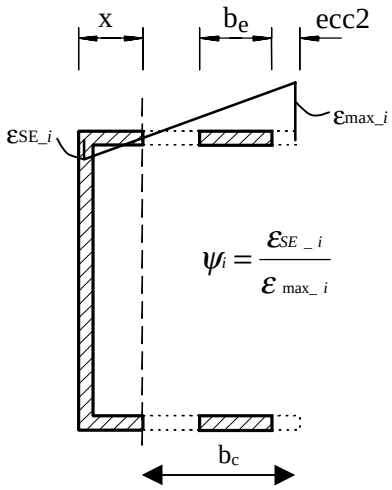

(a) Channel section under strain gradient ψ_i

ε_{FE} = Strain at Free Edge
ε_{SE} = Strain at Supported Edge

$$\psi_i = \frac{\varepsilon_{SE}}{\varepsilon_{FE}}$$

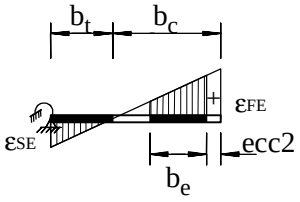

(b) Plate test for strain gradient ψ_i

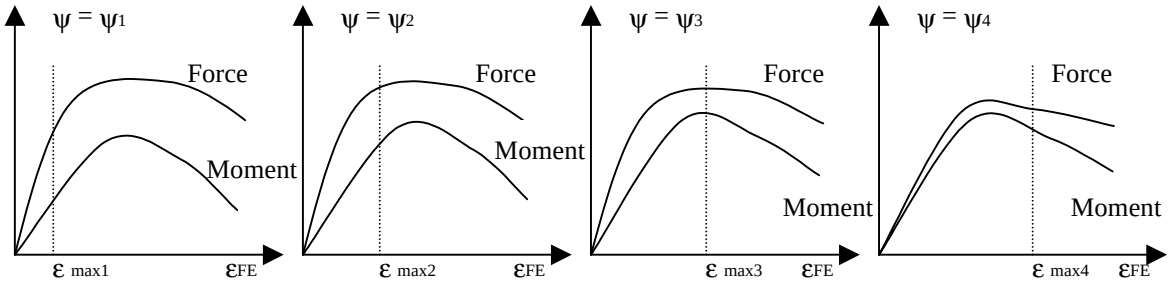

(c) Various plate test results giving values of Force and Moment on the plate against strain at the free edge (ε_{FE}), for particular strain gradients ψ

Figure 1: Exact calculation of the moment capacity of channel sections in minor axis bending using plate test results of unstiffened elements under stress gradients

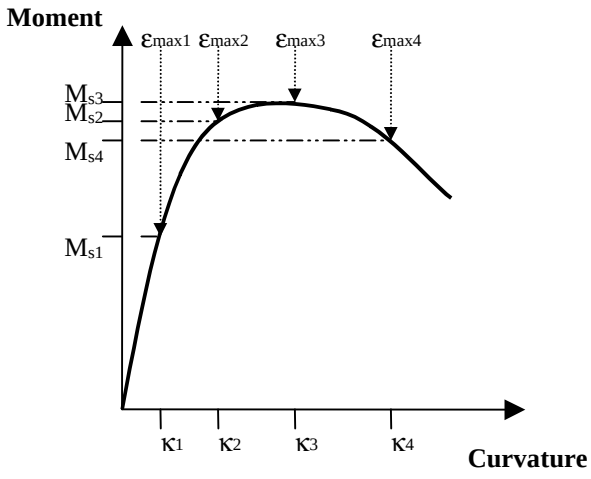

Figure 2: Calculated Moment–Curvature plot for channel section in minor axis bending

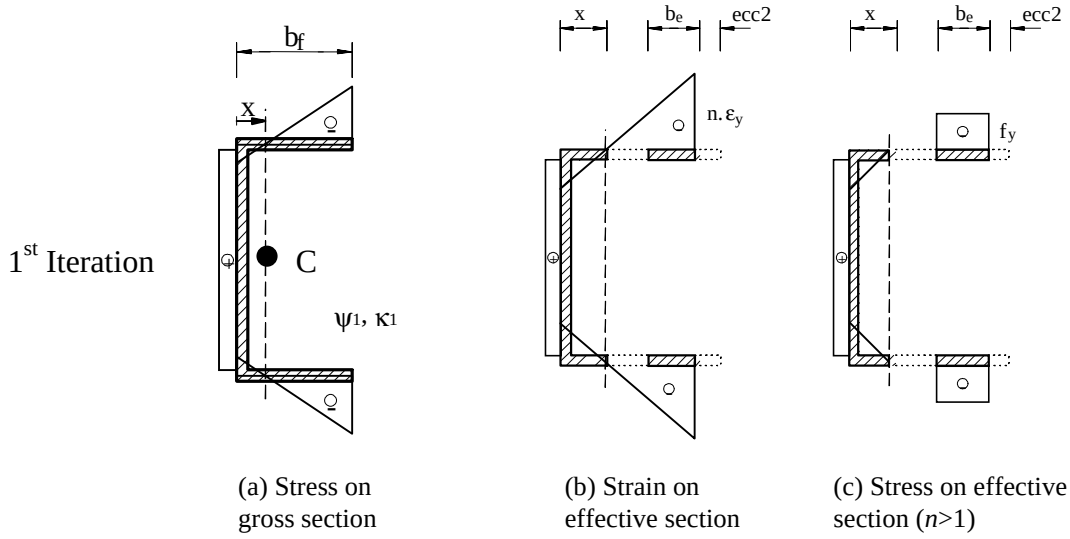

Figure 3: Channel section in minor axis bending, with compression at the unsupported edge of the flange

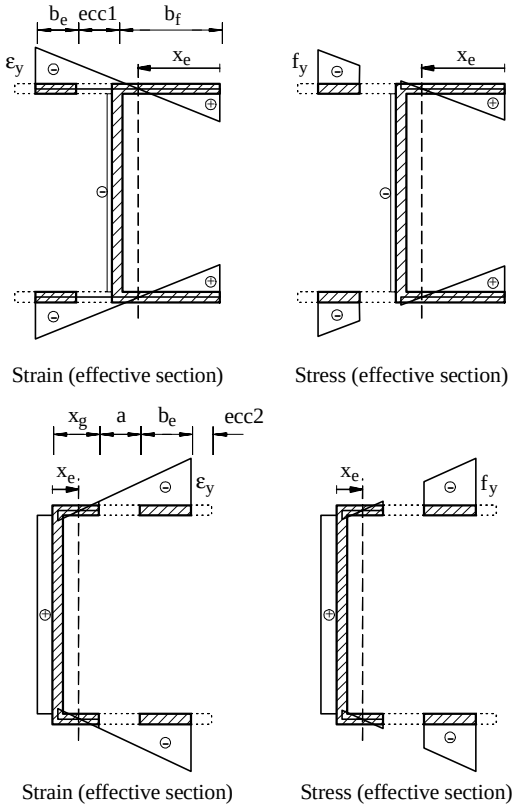

Figure 4: I-sections and channels in minor axis bending – first yield analysis

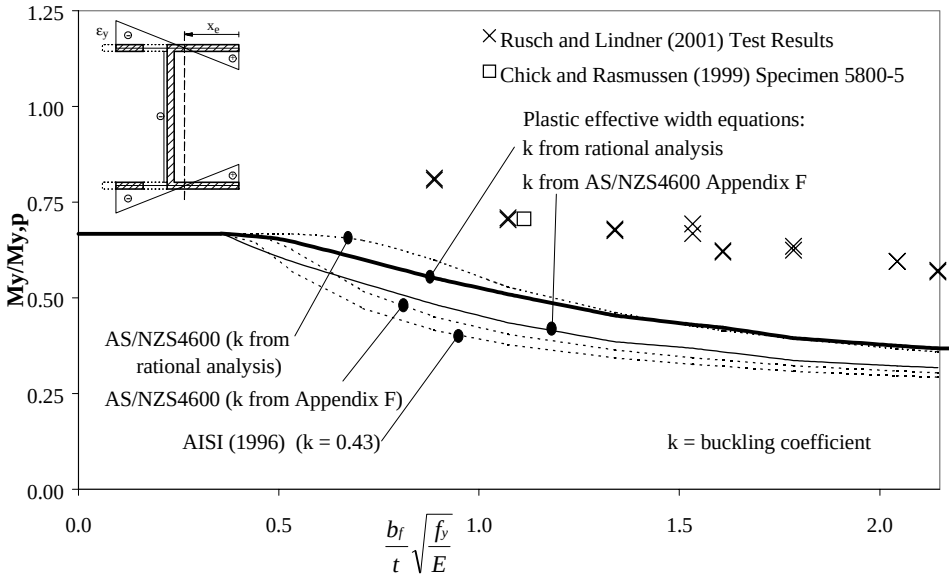

Figure 5: Bending capacities of I-sections using first yield analysis

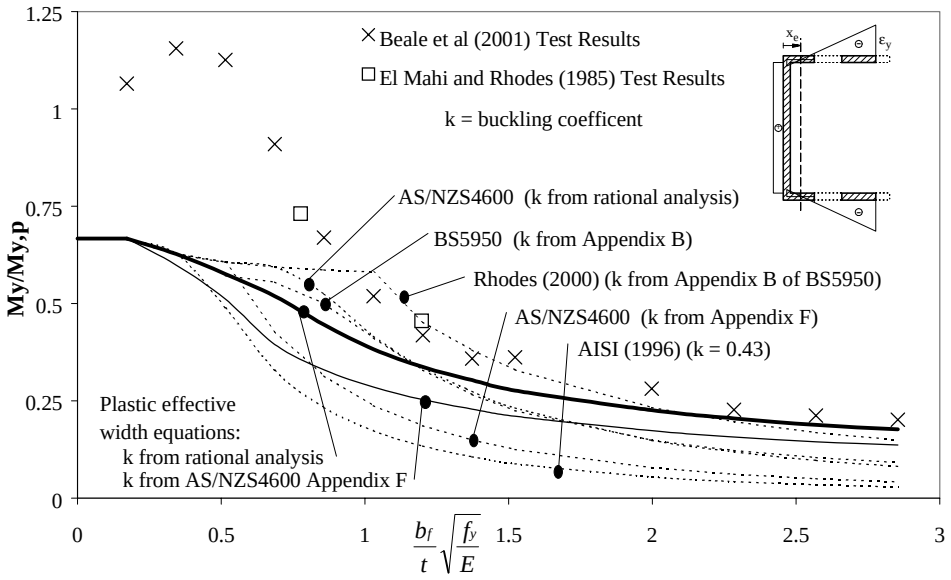

Figure 6: Bending capacities of channels sections using first yield analysis

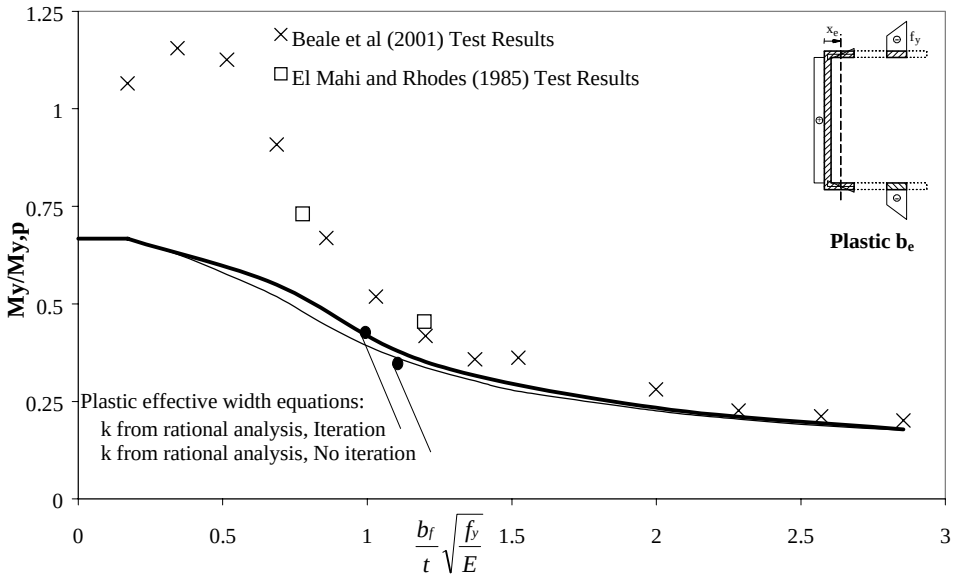

Figure 7: Effect of iterating to establish the effective channel section (using the plastic effective width method)

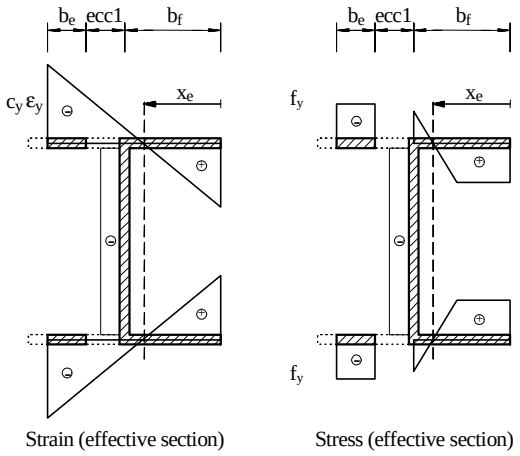

Figure 8: Inelastic reserve capacity - I-sections in minor axis bending

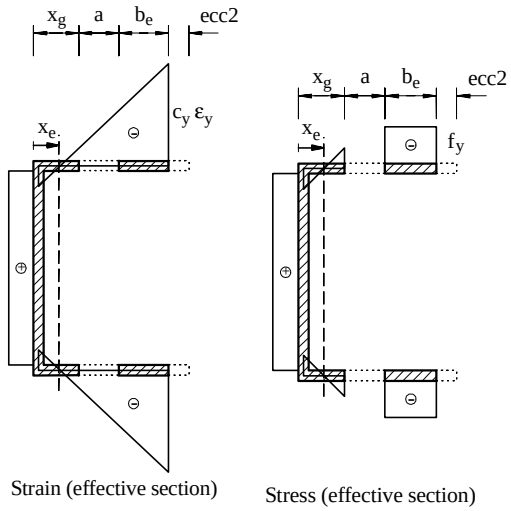

Figure 9: Inelastic reserve capacity - channels in minor axis bending

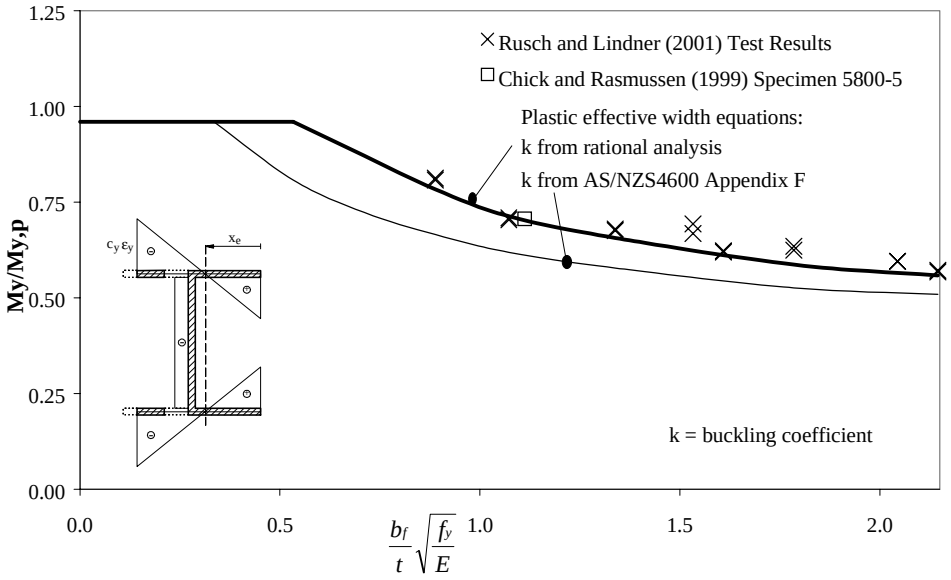

Figure 10 : Bending capacities of I-sections based on inelastic reserve capacity

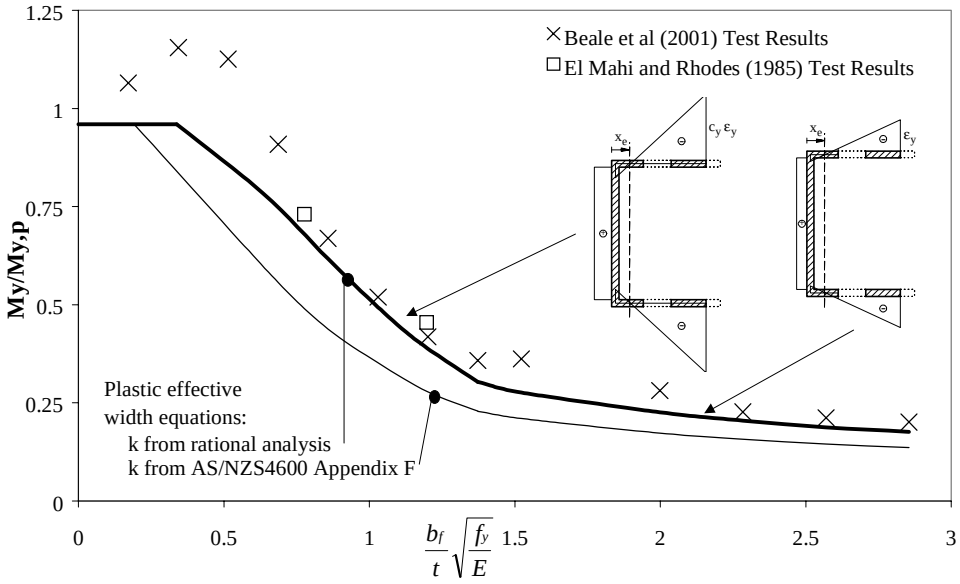

Figure 11: Bending capacities of channel sections based on inelastic reserve capacity

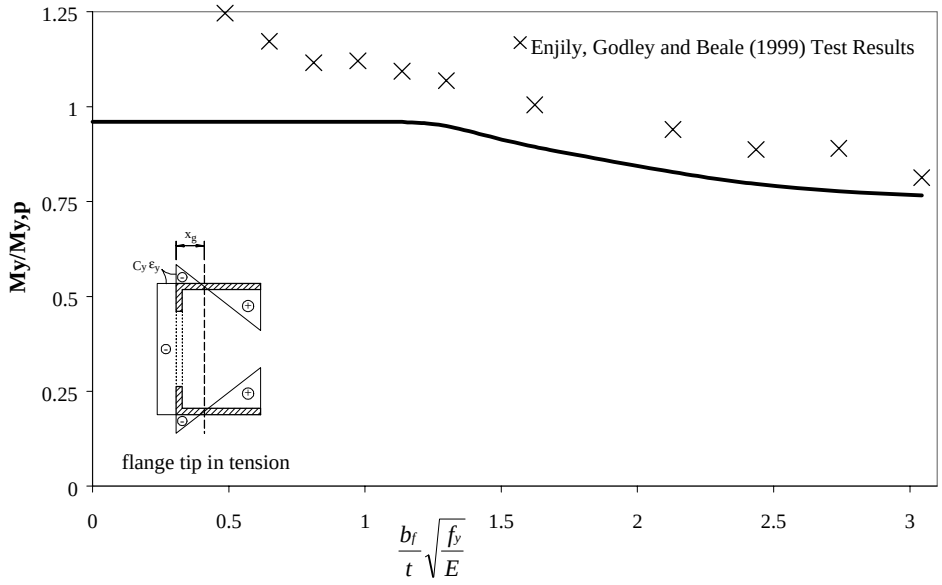

Figure 12: Bending capacities of channel sections based on inelastic reserve capacity

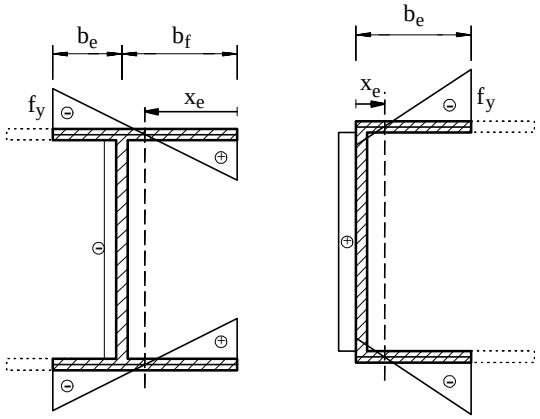

Figure 13: Elastic effective width method

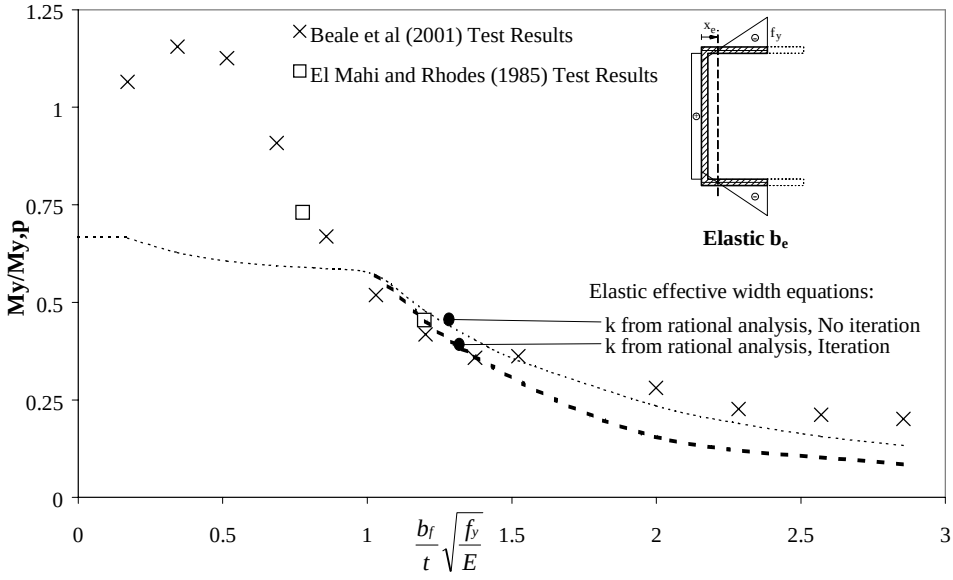

Figure 14: Effect of iterating to establish the effective channel section (using the elastic effective width method)

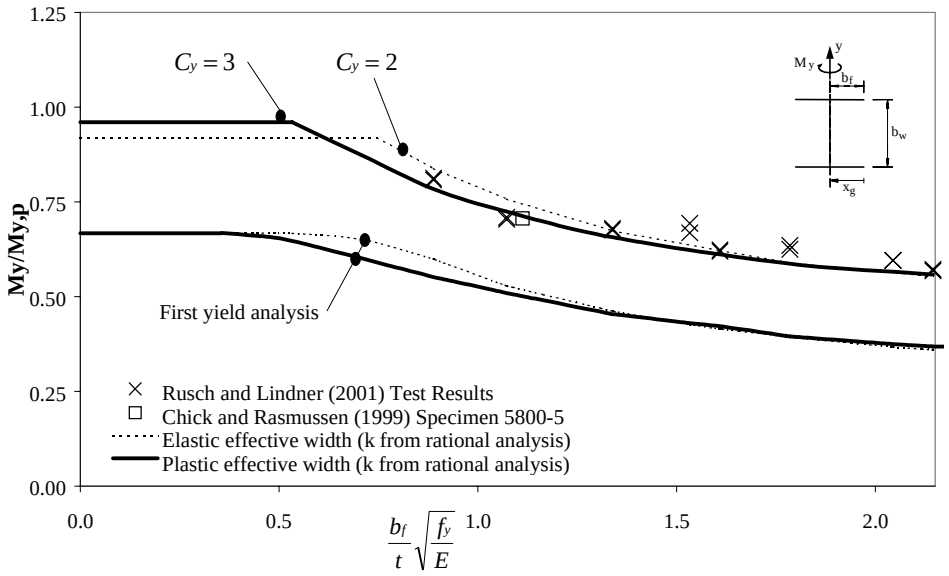

Figure 15: Bending capacities of I-sections using elastic and plastic effective width equations – first yield analysis compared with inelastic reserve capacity

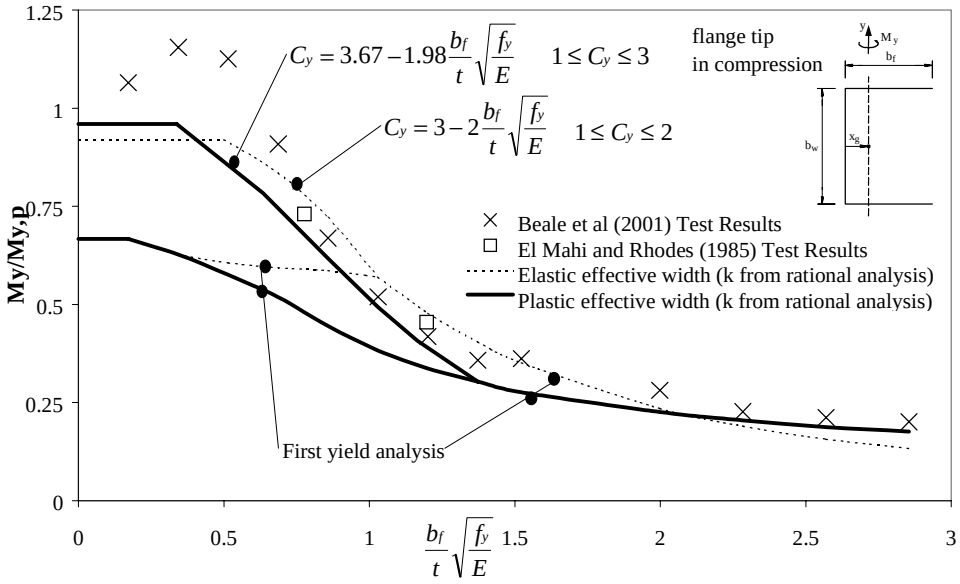

Figure 16: Bending capacities of channels using elastic and plastic effective width equations – first yield analysis compared with inelastic reserve capacity

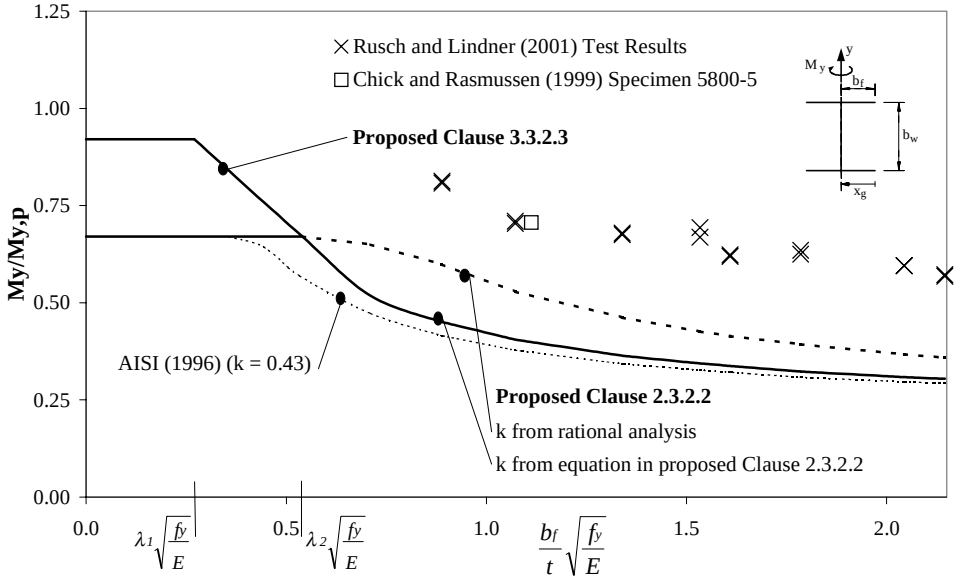

Figure 17: Proposed design model incorporating elastic effective width equations (Clause 2.3.2.2) and an inelastic reserve capacity for fully effective sections (Clause 3.3.2.3), compared with I-section test data

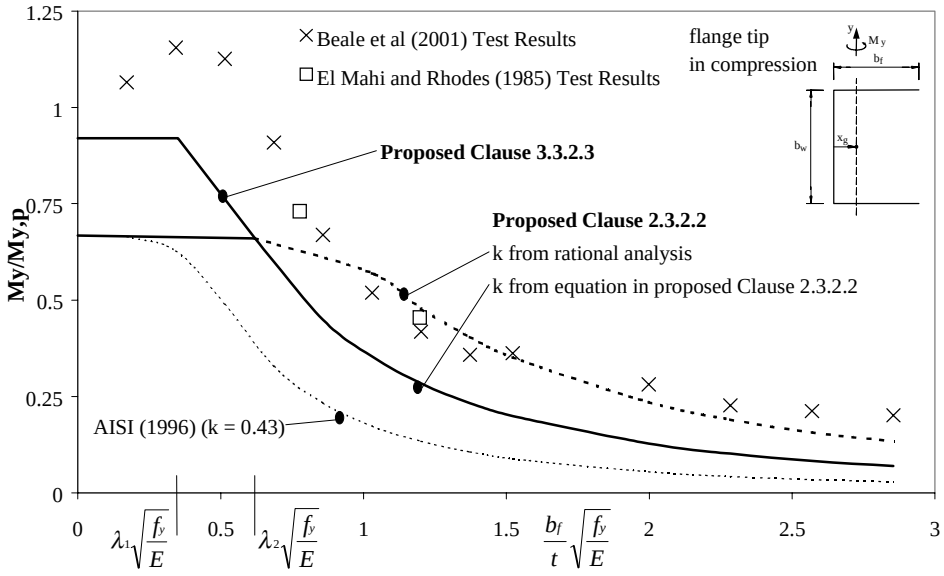

Figure 18: Proposed design model incorporating elastic effective width equations (Clause 2.3.2.2) and an inelastic reserve capacity for fully effective sections (Clause 3.3.2.3), compared with channel section test data

APPENDIX A: MINOR AXIS MOMENT CAPACITY CALCULATIONS

Section properties: $b_f := 50\cdot mm$ $b_w := 80\cdot mm$ $t := 1.9\cdot mm$ $f_y := 228\cdot MPa$ $E := 200000\,MPa$

$$I_y := 4\cdot\left(\frac{t\cdot b_f^{\,3}}{12}+\frac{t\cdot b_f^{\,3}}{4}\right)+\frac{b_w\cdot t^3}{12} \qquad Z_y := \frac{I_y}{b_f} \qquad Z_y = 6.334\cdot 10^3\cdot mm^3$$

$M_y := f_y\cdot Z_y$ $M_y = 1.444\cdot 10^6\cdot N\cdot mm$

$M_{cr} := 2.262\cdot 10^6\cdot N\cdot mm$ calculated from THINWALL

$$\lambda := \sqrt{\frac{M_y}{M_{cr}}} \qquad \lambda = 0.799$$

$$k := \frac{12\cdot 0.91\cdot b_f^{\,2}\cdot f_y}{\lambda^2\cdot t^2\cdot \pi^2\cdot E} \qquad k = 1.368$$ back-calculated from THINWALL

$b_e := b_f\cdot 0.4\cdot\lambda^{-0.75}$ $b_e = 23.665\cdot mm$

$ecc1 := b_f\cdot 0.45$ $ecc1 = 22.5\cdot mm$

$$x_e := \frac{2\cdot b_e\cdot t\cdot\left[\left(2\cdot b_f-\frac{b_e}{2}\right)-\left(b_f-b_e-ecc1\right)\right]+2\cdot b_f\cdot t\cdot\frac{b_f}{2}+b_w\cdot t\cdot b_f}{2\cdot b_e\cdot t+2\cdot b_f\cdot t+b_w\cdot t}$$

$x_e = 46.151\cdot mm$

elastic effective Neutral Axis position

$\varepsilon_y := \frac{f_y}{E}$ $\varepsilon_y = 1.14\cdot 10^{-3}$

$\varepsilon_{max\_eff\_C} := 3\cdot\varepsilon_y$ $x_p := 46.151\cdot mm$

$K := \frac{\varepsilon_{max\_eff\_C}}{b_f-x_p+ecc1+b_e}$ $b_g := \frac{\varepsilon_y}{K}$ $b_p := x_p-b_g$ $\varepsilon_{web} := \left(b_f-\frac{\varepsilon_y}{K}-b_p\right)\cdot K$

$c := b_f-b_g-b_p$ $f_{web} := \varepsilon_{web}\cdot E$ $f_{web} = 52.64\cdot MPa$

$F_T := 2\cdot b_p\cdot f_y\cdot t+b_g\cdot f_y\cdot t$ $F_T = 3.276\cdot 10^4\ N$

$F_C := 2\cdot f_y\cdot b_e\cdot t+\left(b_f-\frac{\varepsilon_y}{K}-b_p\right)\cdot f_{web}\cdot t+b_w\cdot t\cdot f_{web}$ $F_C = 2.889\cdot 10^4\ N$

$$M_s := 2\cdot b_e\cdot t\cdot f_y\cdot\left(ecc1+\frac{1}{2}\cdot b_e+c\right)+2\cdot b_p\cdot t\cdot f_y\cdot\left(x_p-\frac{1}{2}\cdot b_p\right)+\frac{2}{3}\cdot b_g^{\,2}\cdot f_y\cdot t+\frac{2}{3}\cdot c^2\cdot f_{web}\cdot t+b_w\cdot t\cdot f_{web}\cdot c$$

$M_s = 1.697\cdot 10^6\cdot N\cdot mm$

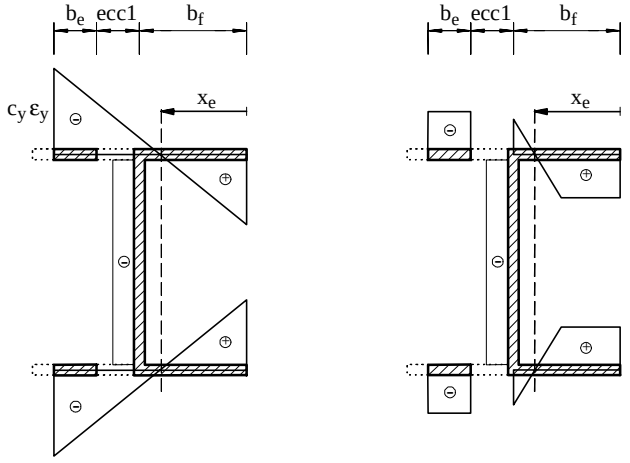

Strain (effective section) Stress (effective section)

Section properties: $b_f := 56\cdot mm$ $b_w := 120\cdot mm$ $t := 1.6\cdot mm$

$E := 200000\,MPa$

$f_y := 232.5\cdot MPa$

$x_g := \frac{b_f^2}{b_w + 2\cdot b_f}$ $x_g = 13.517\,mm$

$\alpha := \frac{-x_g}{b_f - x_g}$ $\alpha = -0.318$

$f_{cr} := 208.2\cdot MPa$ calculated from THINWALL

$\lambda := \sqrt{\frac{f_y}{f_{cr}}}$ $\lambda = 1.057$

$k := \frac{12\cdot 0.91\cdot b_f^2\cdot f_y}{\lambda^2\cdot t^2\cdot \pi^2\cdot E}$ $k = 1.411$ back-calculated from THINWALL

$b_e := b_f\cdot 0.4\cdot(1+\alpha)\cdot\lambda^{-0.75}$ $b_e = 14.653\,mm$

$ecc2 := b_f\cdot\left[0.55\cdot(1+\alpha) - \frac{b_e}{b_f}\right]$ $ecc2 = 6.347\,mm$

$a := b_f - x_g - b_e - ecc2$ $a = 21.483\,mm$

$x_e := \frac{\frac{x_g^2}{2} + 2\cdot b_e\cdot\left(x_g + a + \frac{b_e}{2}\right)}{b_w + 2\cdot x_g + 2\cdot b_e}$ $x_e = 7.553\,mm$ elastic effective Neutral Axis position

$\varepsilon_y := \frac{f_y}{E}$ $\varepsilon_y = 1.162\cdot 10^{-3}$

$C_y := 3.67 - \frac{\frac{b_f}{t}\cdot\sqrt{f_y}}{225\cdot\sqrt{MPa}}$ $C_y = 1.298$

$\varepsilon_{tipc} := C_y\cdot\varepsilon_y$ $x_p := 7.553\cdot mm$

$K := \frac{\varepsilon_{tipc}}{b_f - x_p - ecc2}$ $c := \frac{\varepsilon_y}{K}$ $b_c := x_g - x_p$ $b_p := b_e$

$\varepsilon_{tipt} := K\cdot x_p$ $\varepsilon_{bc} := K\cdot b_c$ $\varepsilon_1 := K\cdot(b_c + a)$

$f_{tipt} := \varepsilon_{tipt}\cdot E$ $f_{bc} := \varepsilon_{bc}\cdot E$ $f_1 := \varepsilon_1\cdot E$

$F_t := x_p\cdot f_{tipt}\cdot t + b_w\cdot f_{tipt}\cdot t$ $F_t = 1.105\cdot 10^4\,N$ $f_{tipt} = 54.146\,MPa$

$F_c := b_c\cdot f_{bc}\cdot t + 2\cdot b_p\cdot f_y\cdot t$ $F_c = 1.131\cdot 10^4\,N$ $f_{bc} = 42.756\,MPa$

$M_s := b_w\cdot f_{tipt}\cdot t\cdot x_p + \frac{2}{3}\cdot x_p^2\cdot f_{tipt}\cdot t + \frac{2}{3}\cdot b_c^2\cdot f_{bc}\cdot t + 2\cdot b_p\cdot f_y\cdot t\cdot\left(b_c + a + \frac{b_p}{2}\right)$

$M_s = 4.625\cdot 10^5\,N\cdot mm$

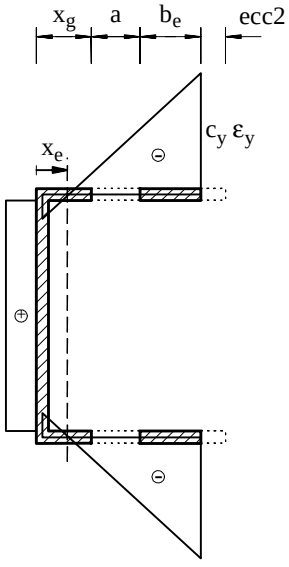

Strain (effective section)

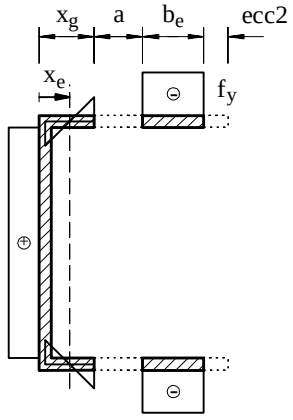

Stress (effective section)

APPENDIX B: PROPOSED AMENDMENTS TO AS/NZS 4600 – EFFECTIVE WIDTH EQUATIONS

2.3.2 Unstiffened elements and edge stiffeners with stress gradient

2.3.2.2 *Effective width for capacity calculations* The following notation is used in this section:

b_e = Effective width measured from the supported edge, determined in accordance with Clause 2.2.1.2 with f^* equal to f_1^* and with k and ρ determined as given in this Clause

f_1^*, f_2^* = Stresses shown in Figures 2.3.2 and 2.3.3 calculated on the basis of the gross section. Where f_1^* and f_2^* are both compression, $f_1^* \geq f_2^*$

ψ = $| f_2^* / f_1^* |$ (absolute value) . . . 2.3.2.2(1)

(a) Unstiffened elements under stress gradient causing compression at both longitudinal edges of the unstiffened element (f_1^* and f_2^* both in compression as shown in Figure 2.3.2)

ρ shall be determined from Equation 2.2.1.2(3)

λ shall be determined from Equation 2.2.1.2(4)

Where the stress decreases toward the unstiffened edge of the element as shown in Figure 2.3.2(a):

$$k = \frac{0.578}{\psi + 0.34} \qquad \text{. . . 2.3.2.2(2)}$$

Where the stress increases toward the unstiffened edge of the element as shown in Figure 2.3.2(b):

$$k = 0.57 - 0.21\psi + 0.07\psi^2 \qquad \text{. . . 2.3.2.2(3)}$$

(b) Unstiffened elements under stress gradient causing compression at one longitudinal edge and tension at the other longitudinal edge of the unstiffened element

For f_1^* in compression at the unsupported edge and f_2^* in tension as shown in Figure 2.3.3(a)

$$\rho = (1+\psi)\frac{\left(1 - \frac{0.22(1+\psi)}{\lambda}\right)}{\lambda} \qquad \rho \leq 1 \qquad \text{. . . 2.3.2.2(4)}$$

λ shall be determined from Equation 2.2.1.2(4)

$$k = 0.57 + 0.21\psi + 0.07\psi^2 \qquad \text{. . . 2.3.2.2(5)}$$

For f_1^* in compression at the supported edge and f_2^* in tension as shown in Figure 2.3.3(b)

For $\psi < 1$ $$\rho = (1-\psi)\frac{\left(1 - \frac{0.22}{\lambda}\right)}{\lambda} + \psi \qquad \rho \leq 1 \qquad \text{. . . 2.3.2.2(6)}$$

λ shall be determined from Equation 2.2.1.2(4)

$$k = 1.70 + 5\psi + 17.1\psi^2 \qquad \text{. . . 2.3.2.2(7)}$$

For $\psi \geq 1$ $\rho = 1$ . . . 2.3.2.2(8)

Alternatively, the plate buckling coefficient (k) in Equations 2.3.2.2(2), 2.3.2.2(3), 2.3.2.2(5) and 2.3.2.2(7) for each flat element may be determined from a rational elastic buckling analysis of the whole section as a plate assemblage subjected to the longitudinal stress distribution in the section prior to buckling.

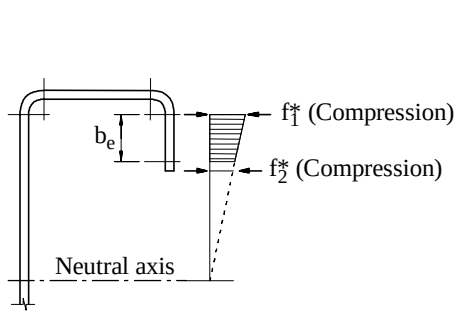

(a) Inward facing lip

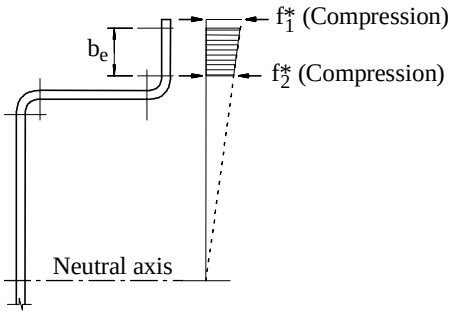

(b) Outward facing lip

FIGURE 2.3.2: UNSTIFFENED ELEMENTS UNDER STRESS GRADIENT, BOTH EDGES IN COMPRESSION

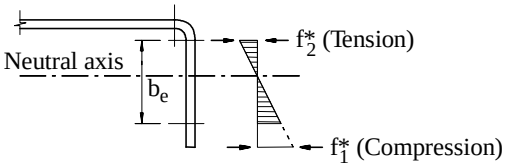

(a) Compression at the unsupported edge

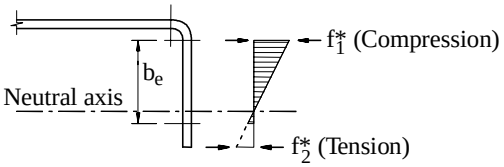

(b) Compression at the supported edge

FIGURE 2.3.3: UNSTIFFENED ELEMENTS UNDER STRESS GRADIENT, ONE EDGE IN COMPRESSION AND ONE EDGE IN TENSION

APPENDIX C: PROPOSED AMENDMENTS TO AS/NZS 4600 – INELASTIC RESERVE CAPACITY

3.3.2 Nominal section moment capacity

3.3.2.2 *Based on inelastic reserve capacity*

(ii) (a) For unstiffened compression elements under stress gradient causing compression at one longitudinal edge and tension at the other longitudinal edge of the unstiffened element:

For $b/t \le \lambda_1$: $C_y = 2$ . . . 3.3.2.3(7)

For $\lambda_1 < b/t < \lambda_2$: $C_y = 2 - [((b/t) - \lambda_1)/(\lambda_2 - \lambda_1)]$ . . . 3.3.2.3(8)

For $b/t \ge \lambda_2$: $C_y = 1$ . . . 3.3.2.3(9)

$$\lambda_1 = \frac{0.27(1+\psi)}{\sqrt{f_y / E}} \quad \text{. . . 3.3.2.3(10)}$$

$$\lambda_2 = \frac{0.54(1+\psi)}{\sqrt{f_y / E}} \quad \text{. . . 3.3.2.3(11)}$$

where ψ shall be determined in accordance with Clause 2.3.2.2

(b) For unstiffened compression elements under stress gradient causing compression at both longitudinal edges of the unstiffened element:

$C_y = 1$

CURRENT AS/NZS4600 (1996)

3.3.2.3 *Based on inelastic reserve capacity* The inelastic flexural reserve capacity may be used if the following conditions are met:

(a) The member is not subject to twisting or to lateral, torsional, distortional or flexural-torsional buckling.

(b) The effect of cold-forming is not included in determining the yield stress (f_y).

(c) The ratio of the depth of the compressed portion of the web (d_w) to its thickness (t_w) does not exceed the slenderness ratio (λ_1).

(d) The design shear force (V^*) does not exceed 0.35 f_y times the web area ($d_1 t_w$).

(e) The angle between any web and the vertical does not exceed 30°.

The nominal section moment capacity (M_s) shall not exceed either $1.25 Z_e f_y$, where $Z_e f_y$ shall be determined in accordance with Clause 3.3.2.1 or that causing a maximum compression strain of $C_y e_y$

where

C_y = compression strain factor

e_y = yield strain

$$= \frac{f_y}{E} \quad \text{. . . 3.3.2.3(1)}$$

E = Young's modulus of elasticity (200×10^3 MPa).

NOTE: There is no limit for the maximum tensile strain.

The compression strain factor (C_y) shall be determined as follows:

(i) For stiffened compression elements without intermediate stiffeners:

For $b/t \le \lambda_1$: $C_y = 3$ . . . 3.3.2.3(2)

For $\lambda_1 < b/t < \lambda_2$: $C_y = 3 - 2[((b/t) - \lambda_1)/(\lambda_2 - \lambda_1)]$ . . . 3.3.2.3(3)

For $b/t \ge \lambda_2$: $C_y = 1$ . . . 3.3.2.3(4)

$$\lambda_1 = \frac{1.11}{\sqrt{f_y / E}} \quad \text{. . . 3.3.2.3(5)}$$

$$\lambda_2 = \frac{1.28}{\sqrt{f_y / E}} \quad \text{. . . 3.3.2.3(6)}$$

(ii) For unstiffened compression elements:

$C_y = 1$

(iii) For multiple-stiffened compression elements and compression elements with edge stiffeners:

$C_y = 1$

If applicable, effective design widths shall be used in calculating section properties. M_s shall be calculated considering equilibrium of stresses, assuming an ideally elastic-plastic stress-strain curve which is the same in tension as in compression, small deformation and that plane sections remain plane during bending. Combined bending and web crippling shall be in accordance with Clause 3.3.7

Replace with:

(c) For Part (i), the ratio of the depth of the compressed portion of the web (d_w) to its thickness (t_w) does not exceed the slenderness ratio (λ_1)

(d) The design shear force (V^*) does not exceed $0.35 f_y$ times the web area ($d_1 t_w$ for (i) and bt for (ii))